

Using projection imaging to study ultracold plasmas

X. L. Zhang, R. S. Fletcher, and S. L. Rolston
*Joint Quantum Institute, Department of Physics,
University of Maryland, College Park, MD 20742*
(Dated: May 29, 2019)

We report a time-of-flight projection imaging technique to study ultracold plasma dynamics. We image the charged particle spatial distribution by extracting them with a high-voltage pulse onto a positive-sensitive detector. Measuring the 2-D Gaussian width of the ion image at later times (the ion image size in the first 20 μs is dominated by the time-of-flight Coulomb explosion of the dense ion cloud), we can extract the plasma asymptotic expansion velocity. The plasma expansion velocities at different initial electron temperatures match earlier results obtained by measuring the plasma oscillation frequency, which provides strong support for this method to study the ultracold plasma dynamics. The electron image size slowly decreases during the plasma lifetime because of the strong Coulomb force of the ion cloud on the electrons, electron loss and Coulomb explosion effects.

PACS numbers: 32.80.Pj, 52.27.Cm, 52.55.Dy, 52.70.Ds

Ultracold plasmas (UCPs), formed by photoionizing laser-cooled atoms near the ionization limit, have well-controlled initial conditions and relatively slow dynamics compared to other laser-produced plasma systems, and thus provide a clean and simple source with excellent spatial and temporal resolution to study basic plasma theory and to explore new physics. Up to now, UCPs are unconfined and freely expanding into surrounding vacuum, a fundamentally important dynamic in laser-produced plasmas as well as UCPs. The expansion dynamics of UCPs are studied experimentally by various methods, such as plasma collective modes [1, 2], absorption imaging [3] and fluorescence imaging [4, 5], and are also studied theoretically by a variety of methods [6, 7, 8, 9].

The first quantitative experimental study of the expansion of UCPs was performed using the plasma collective modes as a probe of the plasma density as a function of time [1]. By applying a small radio-frequency electric field to excite plasma oscillations in a UCP, the plasma density distribution can be mapped from the oscillations, and the ballistic expansion of plasma size is shown to be valid, that is, $\sigma(t) = \sqrt{\sigma_0^2 + v_0^2 t^2}$. For initial temperature ≥ 70 K, the expansion velocity approximately follows $v_0 = \sqrt{\alpha k_B T_e / m_i}$, the ion acoustic velocity due to the electron pressure on the ions, which agrees with a simple hydrodynamics model. At low initial temperature, the UCPs expand faster than expected from a self-similar expansion, which indicates that there are extra heating effects driving the expansion.

The expansion of UCPs can also be studied with optical measurements such as absorption imaging and laser-induced-fluorescence techniques [3, 4]. These methods provide excellent spatial and temporal resolution, and make it possible to follow the entire expansion from plasma formation, through ion acceleration, to final velocity. By using optical absorption imaging technique, the rms ion velocity along the laser beam can be extracted from the width of the absorption images for the

first 20 μs (the signal-to-noise ratio is poor at later times). The rms ion velocities for high initial electron temperatures (> 45 K) agree with expected values from a self-similar expansion of the plasma which assumes adiabatic expansion, that is, neglects the three-body recombination and disorder-induced heating of the electrons. At low initial electron temperatures and high density, electron heating effects (such as three-body-recombination, disorder-induced heating, radiative decay and Rydberg-electron collisions) contribute more significantly and for longer time in similar measurements. By using the laser-induced-fluorescence measurement of ions in expanding UCPs in two dimensions, the expansion can be measured up to 50 μs , and reasonably agrees with a modified version of isothermal fluid model with elliptical symmetry. For initial temperature < 100 K, the plasma expands with more energy than expected from initial electron temperature.

In this work we report a time-of-flight projection imaging technique as a tool to study the UCP dynamics during the full lifetime of the plasma, while the other methods mentioned above focus on the dynamics in the early time (up to the first 50 μs). We image the charged particle (ions or electrons) spatial distribution of an expanding UCP by extracting them with a high-voltage pulse and accelerating them onto a position-sensitive detector. The expansion is self-similar, as the ion (or electron) cloud maintains a Gaussian density profile throughout the lifetime of the plasma. Early in the lifetime of the plasma, the ion image size is dominated by the time-of-flight Coulomb explosion of the dense ion cloud. The image size is at a minimum at about 20 μs and then afterwards increases (the Coulomb explosion effect of the ion cloud is neglectable at this point and afterwards), reflecting the true size of the plasma. We obtain the ion image width by 2D Gaussian fitting of the ion image, and extract the final asymptotic expansion velocity by fitting the linear region of the ion images as a function of time at later times ($>$

20 μs). Assuming that the ion cloud maintains the Gaussian density distribution during the Coulomb explosion phase, we can restore the actual ion cloud size from the ion projection image by excluding the Coulomb explosion effect. The plasma size indeed follows the ballistic expansion as expected from a simple hydrodynamics model throughout the whole lifetime of the plasma. It will only result in a few percent change of the plasma asymptotic expansion velocity by including the restored plasma sizes in the early 20 μs compared to that obtained by only fitting the linear region at later times. The plasma expansion velocity at different initial electron temperatures matches earlier results obtained by measuring the plasma oscillation frequency [1], which provides strong support for this method to study the UCP expansion and previous technique. We can also image the electrons during the lifetime of an UCP by switching the polarity of the high-voltage pulse and the accelerating voltages on the grids. Unlike the ion images, the size of the electron image slowly decreases during the lifetime of UCP because of the strong Coulomb effect of the dense ion cloud on the electrons, electron loss and Coulomb explosion effect. This technique provides a good tool to study the UCP dynamics in a magnetic field, such as expansion and plasma instability.

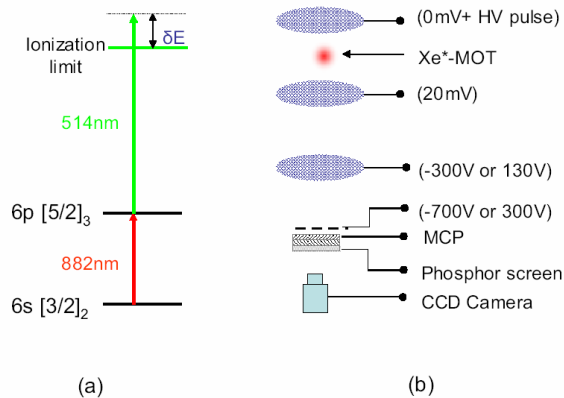


FIG. 1: Two-photon excitation process and experimental setup. (a) two-photon excitation process: one photon (red solid line) at 882 nm drives the $6s[3/2]_2 \rightarrow 6p[5/2]_3$ transition, and the other (10-ns pulse) at 514 nm ionizes the atoms in the $6p[5/2]_3$ state. (b) experimental setup for imaging the charged particles onto the MCP/phosphor screen.

Details of the creation of UCPs are described in [10]. We cooled and trapped about two million metastable Xenon atoms in a magneto-optical trap (MOT) with a temperature of about 20 μK . The spatial density distribution is roughly spherical Gaussian with a rms radius of about 280 μm and a peak density of about $2 \times 10^{10} \text{ cm}^{-3}$. We then produce the plasma by a two-photon excitation

process (figure 1a), ionizing up to 30% of the MOT population. One photon for this process is from the cooling laser at 882 nm to drive the $6s[3/2]_2 \rightarrow 6p[5/2]_3$ transition, and the other is from a pulsed dye laser at 514 nm (10-ns pulse) to ionize the atoms in the $6p[5/2]_3$ state. We control the ionization fraction with the intensity of the photoionization laser, while the initial electron energy is controlled by tuning the 514-nm photon energy with respect to the ionization limit, which is usually in the 1-1000 Kelvin range. Right after the photoionization, the ionized cloud rapidly loses a few percent of the electrons, resulting in a slightly attractive potential for the remaining electrons, and quickly reaches a quasineutral plasma state. It then freely expands with an asymptotic velocity v_0 typically in the 50-100 m/s range caused by the outward electron pressure[1].

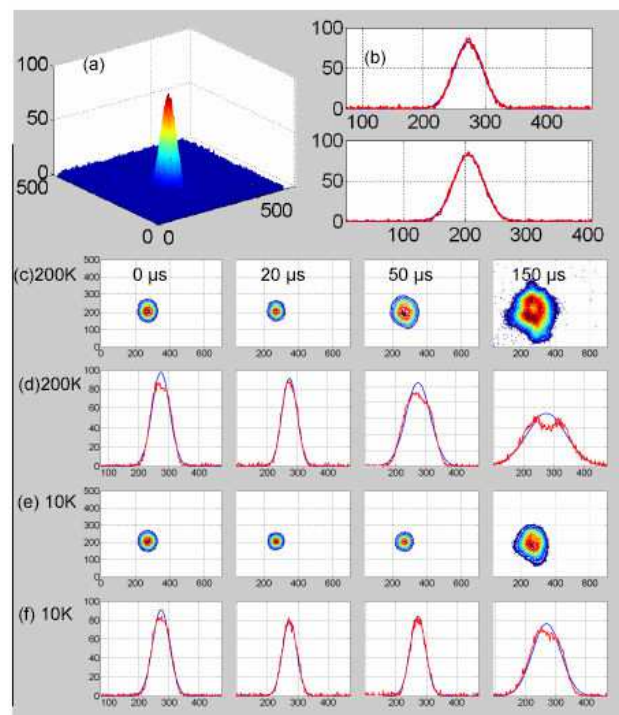


FIG. 2: (a) a false color ion image (2D ion spatial distribution integrated over the third dimension) of an expanding UCP at $t = 20 \mu\text{s}$, $T_e = 100 \text{ K}$; (b) the 2-D Gaussian fittings (blue curves) of the ion image (a) along the x and y axis in the horizontal plane (red curves); (c) and (e) are the contour plots of the ion images at different delay times for $T_e = 200 \text{ K}$ and 10 K , respectively; (d) and (f) are the corresponding 2-D Gaussian fittings of (c) and (e). All the size related units in (a)-(f) are in pixel number, and one pixel unit corresponds to 150 μm . The y axis of (d) and (f) is in arbitrary unit.

For projection imaging of charged particles, external electric fields are applied via four mesh wire grids to direct and accelerate them towards a phase-sensitive detector (a micro-channel plate detector with phosphor screen)

(figure 1b). Two wire mesh grids, usually named top and bottom grids, are about 1.5 cm above and below the plasma, and the other two (named the middle and front grids) are located between the bottom grid and the microchannel plate detector. By applying a high-voltage pulse to the top grid at a specific delay time after the formation of the UCP and with accelerating voltages on the middle and front grids (-300 V and -700 V for ions, 130 V and 300 V for electrons), we image the charged particle distribution of an expanding UCP onto the phosphor screen. The phosphor image, recorded by a CCD camera, is proportional to the charged particle density, and weakly sensitive to their energy. The high-voltage pulse has an amplitude of 340 V for ions (-200 V for electrons), a width of 4 μs , and a rise time of 60 ns. It is accomplished by modifying the square pulse generator used in ion beam deflection in a neutron generator [11], which uses power FETs to fast switch a high voltage source. Figure 2 are typical ion projection images (2D ion spatial distribution intergrated over the third dimension) with averages of 8 images to increase the signal to noise ratio. Unless we mention the specific unit for the ion images and the plasma size, it is in pixels and one pixel corresponds to about 150 μm . Figure 2a is a false color plot of ion image of UCP at the delay time of 20 μs and initial electron temperature T_e of 100 K, which fits well to a 2-D Gaussian profile (figure 2b). The ion images maintain a Gaussian profile during the whole lifetime of the UCP as shown in figure 2c-2f. We notice that the ion image profiles have a flat top and even dip at later times about 150-200 μs (figure 2d and 2f, especially for high initial electron temperatures), and it shows up earlier for higher initial electron temperatures. However, it is unknown what causes the flat top and dip in the center of the ion images.

We extract the plasma size by 2-D Gaussian fitting of the ion images (figure 2c and 2e) at specific delay times after the formation of UCP. Figure 3 is the measured plasma sizes as a function of delayed time for different initial electron temperatures (the first 200 μs). The curves are for initial electron temperatures of 400 K, 200 K, 60 K and 10 K from top to bottom respectively. Early in the lifetime of the plasma, the measured image size is dominated by the strong time-of-flight Coulomb explosion of the dense ion cloud, not the real size of the plasma. This is because the electrons are extracted from the UCPs very quickly in a few nanoseconds by the high voltage pulse, but the ions maintain Gaussian spatial distribution. The ions will then fly to the detector in about 8-9 μs which depends on the high voltage pulse and the accelerating voltages of the other grids (the time-of-flight time of the ions to the detector can be determined from the delay time of the ion current after the formation of the plasma relative to the high-voltage pulse). At early times ($< 20 \mu\text{s}$), the plasma size is still small (on the order of the initial size, about several hundred micrometers) and the

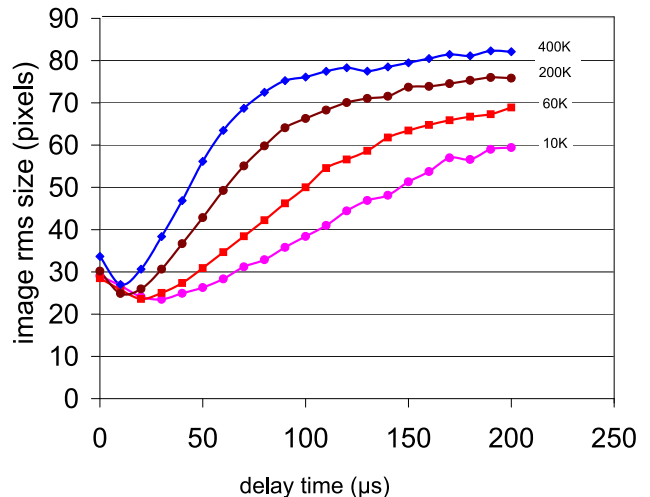


FIG. 3: measured plasma size as a function of elapsed time after the formation of UCP for different initial temperatures. The curves are for initial electron temperatures of 400 K, 200 K, 60 K and 10 K from top to bottom, respectively. Early in the lifetime of the plasma, the size of the image is dominated by the Coulomb explosion of the dense ion cloud.

strong coulomb repulsion between the ions produces a large ion image during the ions transport to the phosphor screen detector. As the plasma size increases, the Coulomb explosion effect diminishes and has less effect on the measured image size (note decreasing images at early times). The image size is at a minimum at about 20-30 μs and afterwards increases, reflecting the true size of the plasma with a constant magnification factor of 1.3 (discussed below), as expected from the ballistic expansion model. The size increases slowly and the minimum point of the measured plasma size moves to a later time as we decrease the initial electron temperature, because the expansion velocity which depends on the initial electron temperature gets smaller as we decrease the electron temperature, and also the Coulomb explosion effect will diminish slowly because of the slower expansion.

Assuming that the ion cloud will be not affected by the fast high-voltage pulse and maintain spherical Gaussian distribution during the ions transport to the detector, we can extract the initial ion cloud size from the ion projection image by excluding the Coulomb explosion effect. This is done as following: First, we start with the plasma density distribution $n(r, t) = n_0(\sigma_0/\sigma_t)^3 e^{-r^2/(2\sigma_t^2)}$, where σ_t follows the ballistic expansion; then, we calculate the Coulomb potential of the ion cloud at specific delay time and extract the average acceleration of the ion cloud; next, we obtain the ion cloud size and expansion velocity after the Coulomb explosion with a small time-of-flight step (small enough for constant acceleration for each iteration); finally, we iterate this procedure to get the final ion cloud size af-

ter the total 8-9 μs time-of-flight, which agrees with the measured ion size. that is, the plasma size indeed follows the ballistic expansion as expected from a simple hydrodynamics model throughout the whole lifetime of the UCP. This will only result in about a few percent change in the plasma expansion velocity by including the restored plasma sizes of the early time compared to that by only fitting the linear region of the ion image sizes at later time. If we also consider that the ion cloud will freely expand with the ion acoustic velocity in addition to the Coulomb explosion during the 8-9 μs time-of-flight time, we need to shift the plasma sizes up by several hundred micrometers, which is equivalent to shifting the x-axis (time) in figure 3 by that amount of time, but this does not affect the overall slope of the plasma size's temporal evolution, that is, the plasma expansion velocity. At later times, especially for high initial electron temperatures, the measured size does not linearly increase. This is partly because the size of the UCP is large enough to be affected by the 4 posts that secure the mesh wire grids above and below the plasma (the top and bottom grids), and it reaches the size of the phosphor screen which is about 3 cm in diameter.

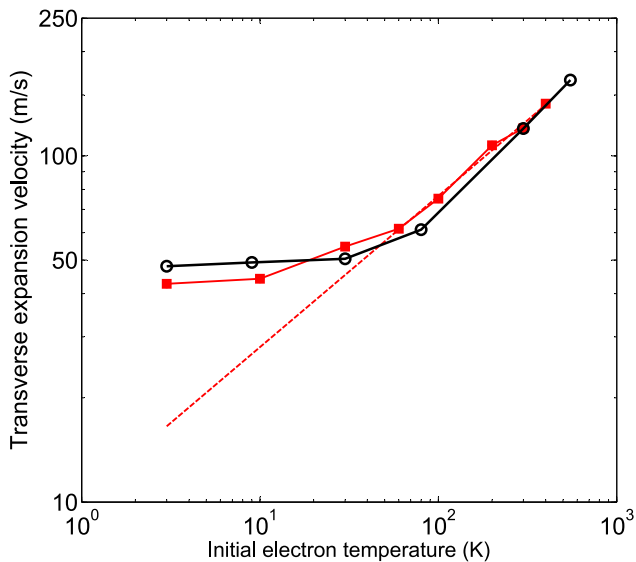


FIG. 4: The asymptotic expansion velocity as a function of initial electron temperature T_e . The red solid line with square points is the experimental result which matches the results obtained by measuring the plasma oscillation frequency (the black solid curve with circle points)[1]. The red dashed line is the linear fitting of the data above 60 K with a slope of about 1/2.

By linear fitting to the sizes after about 20 μs (for high initial electron temperatures, only fitting the restricted linear region), we can get the asymptotic expansion velocities of UCP at different initial electron temperatures with a magnification factor of about 1.3 due to the ions lensing effect (the red solid curve with square points in figure 4).

The ion lensing effect comes from the electric fields which tend to focus or expand the ions beams (depends on the voltage settings of the grids) as they transport to the phosphor screen detector. It is confirmed by adjusting the voltages on the grids (especially the middle and front grids between the bottom grid and the detector), which strongly affect the ion image size as well as the scaling factor. By using SIMION 3D, a popular ion optics simulation program designed to study and analyze ion optics, we can simulate our ion projection imaging setup with the actual spacings and voltage settings of the grids, and get the ion lensing factor from the trajectories (which is about 1.3 for the images at figure 2). At high initial electron temperatures (≥ 60 K), the expansion velocities v_0 is proportional to $\sqrt{\alpha T_e}$ as expected from a simple hydrodynamics model, that is, the slope of the red dashed line in figure 4 is about 1/2; at lower initial electron temperature (≤ 60 K), the expansion velocities are higher than expected from the self-similar expansion, which indicates extra heatings for the expansion at low initial electron temperatures. The black solid line with triangle points is the asymptotic expansion velocity obtained by measuring the plasma oscillation frequency [1]. The good agreement between our experimental results and earlier results by measuring the plasma oscillation frequency [1] strongly supports the measurement of UCP expansion velocity by using the time-of-flight projection imaging method and previous technique.

Many authors addressed the problem of the additional heating effects of the ultracold plasma at low initial electron temperatures in a series of theory papers pointing to the continuum lowering, disorder-induced heating, and three-body recombination (TBR) as sources of electron heatings. TBR dominates in ultracold neutral plasmas because the total TBR rate varies with temperature as $T^{-9/2}$. Reference [12] shows experimental evidence of TBR in an ultracold neutral plasma. By inclusion of TBR and electron-Rydberg-atom collisions, the enhanced expansion velocity at low initial electron temperature can be reproduced by a simple hydrodynamic model with standard collision rates [13].

Using the same technique, we can also image the electrons onto the phosphor screen by reversing the polarity of the high voltage pulse and the voltages on the grids between the plasma and detector. Figure 5 is the measured electron size as a function of elapsed time after the formation of UCP. The black curve with dot points is the measured electron size extracted from the 2D Gaussian fitting of the electron images. The brown curve with triangle points are the electron size with the actual scaling factor due to the electron lensing effect, which is consistent with the theoretical calculation electron size with 100 ns Coulomb explosion time (the red curve with unfilled square points), which was also taken into account the electron loss due to the evaporation of electrons out of the system. We assume that the ion cloud follows a

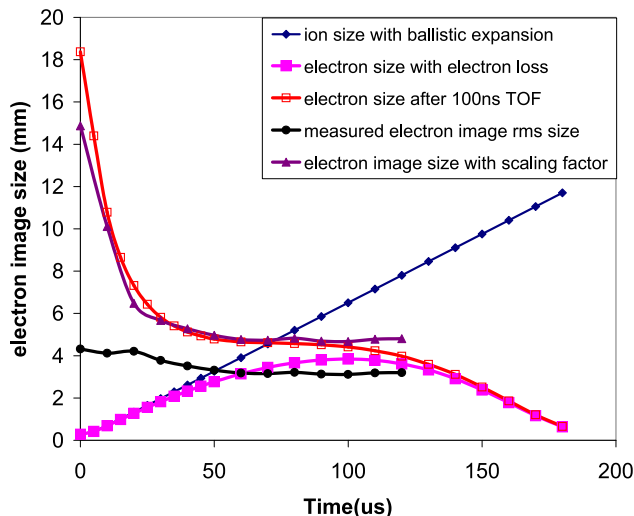


FIG. 5: The electron sizes of UCPs as a function of time for $T_e = 100$ K. The black curve with dot points is the electron size extracted from the 2D Gaussian fitting of the electron images. The brown curve with triangle points are the electron size with the scaling factor due to the charged particle lensing effect, which is consistent with the theoretical calculation electron size with 100 ns Coulomb explosion time (the red curve with unfilled square points).

ballistic expansion model (the blue curve with diamond points), while the electron distribution is initially identical to the ion distribution, but with a truncation at the appropriate radius such that the total electron number agrees with the measured charge imbalance at a specific delay time. We then perform self-consistent calculations for the plasma potential to extract the final electron size (the magenta curve with square points) [14]. The electron lensing factor is obtained from the SIMION 3D trajectory simulation with the actual voltage settings of the grids, the actual spacings between the grids and detector, and the ion spatial distribution. We should point out that the electron lensing factor, unlike that of the ions, is not a constant number during the whole UCP lifetime due to the strong coulomb force of the ion cloud on the much lighter electrons, especially for the first $30 \mu\text{s}$. The electrons are removed from the plasma in a few nanoseconds after applying the high-voltage pulse, but the ions maintain their Gaussian spatial distribution during that short period of time, which will exert a strong Coulomb force on the electrons and partially cancel the applied electric field. This will increase the electron lensing factor, confirmed by the SIMION trajectory simulation. As the plasma expands, the plasma size gets larger, and the Coulomb force on the electrons due to the ion cloud gets

smaller, so the electron lensing factor towards constant at later time (after $30 \mu\text{s}$). The ion lensing factor is constant because there are no electrons left during the ion Coulomb explosion phase.

In conclusion, we have described the use of time-of-flight projection imaging technique to study the ultracold plasma dynamics such as plasma expansion. Unlike the previous experimental technique which can only study the dynamics in the early time of the ultracold plasma evolution, this method can study the UCP expansion dynamics in the whole lifetime. The plasma expansion velocity at different initial electron temperatures has good agreement with the previous results by different technique. This powerful method is useful for further study the ultracold plasma dynamics in a magnetic field in the whole lifetime, such as plasma instability, plasma expansion and magnetic confinement.

This work was partially supported by the National Science Foundation PHY-0245023 and PHY-0714381.

-
- [1] S. Kulin, T. C. Killian, S. D. Bergeson, and S. L. Rolston, *Phys. Rev. Lett.* **85**, 318 (2000).
 - [2] R. S. Fletcher, X. L. Zhang, S. L. Rolston, *Phys. Rev. Lett.* **96**, 105003 (2006).
 - [3] C. E. Simien, Y. C. Chen, P. Gupta, Y. N. Martinez, P. G. Mickelson, S. B. Nagel, and T. C. Killian, *Phys. Rev. Lett.* **92**, 143001 (2004).
 - [4] E. A. Cummings, J. E. Daily, D. S. Durfee, and S. D. Bergeson, *Phys. Rev. Lett.* **95**, 235001 (2005).
 - [5] E. A. Cummings, J. E. Daily, D. S. Durfee, and S. D. Bergeson, *Phys. Plasmas* **12**, 123501 (2005).
 - [6] S. D. Bergeson, R. L. Spencer, *Phys. Rev. E* **67**, 026414 (2003).
 - [7] F. Robicheaux and J. D. Hanson, *Phys. Plasmas* **10**, 2217 (2003).
 - [8] T. Pohl, T. Pattard, and J. Rost, *Phys. Rev. Lett.* **92**, 155003 (2004).
 - [9] S. Mazevet, L. collins, and J. D. Kress, *Phys. Rev. Lett.* **88**, 055001 (2002).
 - [10] T. C. Killian, S. Kulin, S. D. Bergeson, L. A. Orozco, C. orzel, and S. L. Rolston, *Phys. Rev. Lett.* **83**, 4776 (1999).
 - [11] D. Tomic, *Rev. Sci. Instrum.* **61**, 1729 (1990).
 - [12] T. C. Killian, M. L. Lim, S. Kulin, R. Dumke, S. D. Bergeson, S. L. Rolston, *Phys. Rev. Lett.* **86**, 3759 (2001).
 - [13] F. Robicheaux and J. D. Hanson, *Phys. Rev. Lett.* **88**, 55002 (2002).
 - [14] R. S. Fletcher, *Three-body Recombination and Rydberg Atoms in Ultracold Plasmas* (PhD thesis, University of Maryland, 2008).